
QUASI ZIGZAG PERSISTENCE: A TOPOLOGICAL FRAMEWORK FOR ANALYZING TIME-VARYING DATA

A PREPRINT

Tamal K. Dey
Department of Computer Science
Purdue University
West Lafayette, IN
tamaldey@purdue.edu

Shreyas N. Samaga
Department of Computer Science
Purdue University
West Lafayette, IN
ssamaga@purdue.edu

February 25, 2025

ABSTRACT

In this paper, we propose Quasi Zigzag Persistent Homology (QZPH) as a framework for analyzing time-varying data by integrating multiparameter persistence and zigzag persistence. To this end, we introduce a stable topological invariant that captures both static and dynamic features at different scales. We present an algorithm to compute this invariant efficiently. We show that it enhances the machine learning models when applied to tasks such as sleep-stage detection, demonstrating its effectiveness in capturing the evolving patterns in time-evolving datasets.

1 Introduction

Time varying data analysis Hamilton (1994); Box & Jenkins (1976) has been a fundamental challenge in the machine learning community for a long time, ranging from traditional univariate and multivariate time-series data to more complex structure such as sequence of graphs or point clouds. While the traditional time-series data has been handled effectively Wu et al. (2020), increasing complexity of modern applications has necessitated novel methodologies. Spatiotemporal Graph Neural Networks Yu et al. (2018); Oreshkin et al. (2021); Kan et al. (2022); Chu et al. (2023) have emerged as powerful tools to analyze graph sequences by decomposing the problem into two components: spatial dependency and temporal evolution. Similarly, specialized architectures have been proposed to process sequences of point clouds Liu et al. (2019); Fan et al. (2021); Huang et al. (2021); Rempe et al. (2020). However, most of these approaches utilize the geometric information, which is mostly local, among other information potentially missing crucial global patterns in the data. This becomes apparent in scenarios where the overall shape and connectivity of the data carry significant meaning, such as in brain connectivity patterns. Topological methods offer a compelling solution by capturing these global structures that persist across different scales. By augmenting the models with topological information, we can develop models that leverage both local geometric patterns and global topological characteristics for improved performance.

Recently, topological Data Analysis (TDA) has emerged as a prominent field that can leverage topological information hidden behind the data into its analysis. Persistent Homology (PH), a cornerstone of TDA, provides a succinct method to extract and represent *multiscale* topological information. This capability has proved transformative in enhancing machine learning models, particularly where topological properties carry relevant information Corbet et al. (2019); Chen et al. (2019); Carrière et al. (2020); Kim et al. (2020); Gabrielsson et al. (2020); Hofer et al. (2020); Zhao et al. (2020); Swenson et al. (2020); Carrière & Blumberg (2020); Vipond (2020); Bouritsas et al. (2022); Horn et al. (2022); Cang & Wei (2017); Zhang et al. (2022); Liu et al. (2022); Lesnick & Wright (2015). Time-varying data needs extensions of the classical one-parameter persistence homology along two directions. First, the temporal component of the data necessitates another parameter, thus bringing multi parameter persistence homology (MPH) into picture. Second, monotone filtrations usually associated with the standard PH computations cannot accommodate deletions that are required for processing time-varying data. This necessitates to use zigzag persistent homology (ZPH) which has been shown to capture dynamic topological features in time-series data Myers et al. (2023); Chen et al. (2021);

Tinarrage et al. (2025). In effect, we need a combination of MPH and ZPH which allows PH (standard filtration) along one parameter and ZPH along the other. This requires changes to the structure of the underlying partially-ordered set (poset) to what we call *quasi-zigzag poset* resulting into *Quasi Zigzag Persistent Homology* (QZPH) introducing additional complexity and a new set of challenges.

While MPH captures richer topological information than PH, it presents a different set of challenges due to lack of a complete invariant. This has motivated TDA researchers to look for different invariants that, although not complete, capture sufficient topological information Vipond (2020), Corbet et al. (2019); Carrière & Blumberg (2020); Scoccola et al. (2024); Loiseaux et al. (2023); Xin et al. (2023); Mukherjee et al. (2024). The juxtaposition of ZPH to MPH needs the zigzag generalizations of these methods.

In this paper, we find that, one of these methods called GRIL Xin et al. (2023) that computes a landscape function Bubenik (2015) using generalized ranks of intervals Kim & Mémoli (2021) adapts naturally to the framework of QZPH both conceptually and computationally. This adaptation leads to our key contribution which we call ZZ-GRIL, a new topological invariant that extends GRIL Xin et al. (2023) framework to capture multiscale topological information in time-evolving data. On the theoretical front, we prove the stability of ZZ-GRIL and show that the generalized rank of a specific type of subposet, in the setting of QZPH, can be computed by an algorithm presented in Dey et al. (2024). We use this to devise an algorithm to compute ZZ-GRIL, making this method practical for real-world applications. We demonstrate the practical value of ZZ-GRIL by experimenting on data from critical healthcare monitoring tasks, such as sleep-stage detection via ECG and multivariate time-series data from other applications. We augment the topological information captured by ZZ-GRIL with existing machine learning models and show that the addition of topological information improves the performance of the models as exhibited by experimental results in Section 5¹.

In a very recent paper Flammer & Hüper (2024), the authors consider a similar setup and develop a method to visualize such data using *spatiotemporal persistence landscapes*. We acknowledge that the setup is similar but there are many differences in the overall results. One main difference is that Flammer & Hüper (2024) uses rectangles as intervals that allow them to use a simple modification of a result in Dey et al. (2024) whereas we use more general subposets for which we prove Theorem 4.5, which allows us to compute generalized ranks with zigzag modules. Because of the same reason, the overall algorithm to compute the landscape also becomes different. Additionally, we give an efficient algorithm to build a quasi zigzag bi-filtration from an input time-varying data. Finally, we develop a complete ML pipeline that we experiment with real world time-varying data which is not considered in Flammer & Hüper (2024).

2 Overview

We begin by recalling the definition of a simplicial complex. Given a finite vertex set V , a simplicial complex $K = K(V)$ is a collection of subsets of V such that if a subset $\sigma \subseteq V$ is in K , then all subsets $\tau \subset \sigma$ are also in K . Each element in K with cardinality $k + 1$ is called a k -simplex or simply a simplex. A (non-zigzag) *filtration* \mathcal{F} is a nested sequence of simplicial complexes indexed by integers/natural numbers: $\mathcal{F} : K_0 \hookrightarrow K_1 \hookrightarrow \dots \hookrightarrow K_n$ where the inclusion arrows are all in forward direction. If these arrows are not all in forward direction, we get a filtration called *zigzag filtration*

$$\mathcal{Z} : K_0 \hookrightarrow K_1 \leftarrow \dots \hookrightarrow K_n.$$

Extending the indexing to two parameters such as a grid of integers \mathbb{Z}^2 , we get a bi-filtration (possibly zigzag). We will be interested in a bi-filtration where the filtration in one direction, say y -direction, is non-zigzag and the filtration in the other, x -direction, is zigzag. For a moving point cloud data (PCD) such filtrations arise naturally. For example, consider the case in Figure 1. The moving PCD with 3 points are shown at the bottom row. Along the y -direction, we increase the threshold $\delta > 0$ so that any two points are joined by an edge if the distance between them is no more than δ . Then, along y -direction, for every PCD, we get a non-zigzag filtration whereas along x -direction, for every fixed δ , we get a zigzag filtration. We call this mixing of zigzag and non-zigzag a *quasi zigzag bi-filtration*.

From such a quasi zigzag bi-filtration, we obtain a so-called *persistence module* by considering the simplicial homology group $H_p(K_i)$ in some dimension p for every simplicial complex K_i . The inclusion maps in zigzag or non-zigzag filtrations translate to homomorphisms among these homology groups which become linear maps when homology groups turn into vector spaces under a field coefficient, say k . These vector spaces with dimension, say d , are often depicted with their isomorphic counterparts of d copies of k , written as k^d . We refer to such a persistence module as a *quasi zigzag persistence module*; In Figure 1 (right), we show the quasi zigzag persistence module for zeroth homology group $H_0(\cdot)$ that represents the number of components.

¹Code is available at <https://github.com/TDA-Jyamiti/zzgril>

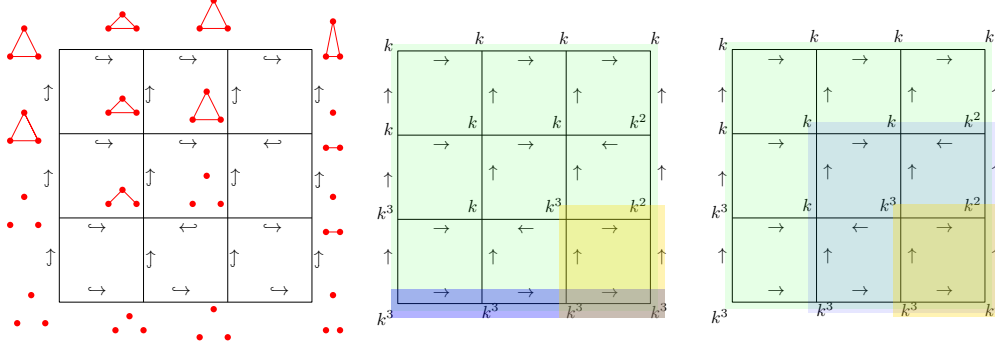


Figure 1: (left) A PCD (bottom row) and a resulting quasi zigzag bi-filtration; (middle) corresponding quasi zigzag persistence module and three intervals (light blue, yellow, green); (right) a rectangle (light yellow) is expanded for obtaining landscape width.

The indexing set of a non-zigzag, zigzag, or quasi zigzag filtration can be thought of as a poset P where for every pair of comparables $\mathbf{p} \leq \mathbf{q}$ in P , one has the inclusion of complexes $K_{\mathbf{p}} \subseteq K_{\mathbf{q}}$. A non-zigzag poset can be indexed by integers in \mathbb{Z} . A zigzag poset that arises in our case is a subset of the poset $\mathbb{Z}\mathbb{Z}$ defined below.

Definition 2.1 ((Quasi) Zigzag Poset). Let $\mathbb{Z}\mathbb{Z}$ be the subset of $\mathbb{Z}^{\text{op}} \times \mathbb{Z}$ defined as

$$\mathbb{Z}\mathbb{Z} := \{(i, j) : i \in \mathbb{Z}^{\text{op}}, j \in \{i, i-1\}\}.$$

A poset P is called *zigzag* if P is a subset of $\mathbb{Z}\mathbb{Z}$ and is *quasi zigzag* if it is a subset of the product $\mathbb{Z}\mathbb{Z} \times \mathbb{Z}$ with the product order.

Now, we formally define persistence modules over different kind of posets.

Definition 2.2 (Persistence module). A persistence module M over a poset P is a functor $M : P \rightarrow \text{vec}$ where P is considered as a category and vec is the category of finite dimensional vector spaces. Stating more explicitly, M is a collection of vector spaces $\{M_{\mathbf{p}}\}_{\mathbf{p} \in P}$ and linear maps $\{M_{\mathbf{p} \rightarrow \mathbf{q}}\}$ for every comparable $\mathbf{p} \leq \mathbf{q}$ in P . It is called a *zigzag module* if P is zigzag and a *quasi zigzag module* if P is quasi zigzag.

Next, we introduce the concepts of *connectedness* and *intervals* in posets which will be used for further exposition. We say a poset P is *connected* if there is a sequence of points $p = r_1, \dots, r_t = q$ in P so that $r_i \leq r_{i+1}$ or $r_{i+1} \leq r_i$ for every $i \in \{1, \dots, t-1\}$. We say a subset $I \subseteq P$ is *convex* if for every pair $p, q \in I$ and every $p \leq r \leq q$, we have $r \in I$. An *interval* I in a poset P is subset which is both convex and connected. An interval I with $m \geq 0$ minima and $n \geq 0$ maxima is called an (m, n) -interval. In the special case of \mathbb{Z}^2 , every interval has a special form where the sets of minima and maxima along with other points constitute staircases that can be visualized as part of the boundary of the interval; see Figure 2.

The main construct upon which we build ZZ-GRIL involves the so-called *generalized ranks* Kim & Mémoli (2021) which can be computed efficiently by a zigzag persistence algorithm Dey et al. (2024). Let P be a quasi zigzag poset over which a quasi zigzag persistence module M is defined and $I \subseteq P$ be a subset. When M is induced by a bi-filtration in QZPH, the generalized rank of the module restricted to I measures the multiplicity of the homological features (# of independent homological classes) that have support over the entire poset I . For example, considering $I = P$ (shaded light green), we see that, in Figure 1(middle), one component survives the entire poset. Then, its generalized rank for zero-th homology H_0 is 1. Similarly, the subset in the bottom row (light blue) has a generalized rank of 3 for H_0 and the subset in bottom right square (light yellow) has a generalized rank of 2 for H_0 . We formally define generalized rank below.

Definition 2.3 (Generalized rank). Let $M : P \rightarrow \text{vec}$ be a persistence module from a finite and connected poset P . The restriction of M to a subset I of P , $M|_I$, is the collection of vector spaces $M_{\mathbf{p}}$ for $\mathbf{p} \in I$ along with linear maps $M_{\mathbf{p} \rightarrow \mathbf{q}}$ for all comparable $\mathbf{p} \leq \mathbf{q}$ in I . Then, the *generalized rank* of M over I is defined as the rank of the canonical linear map from $\lim M|_I$ to $\text{colim} M|_I$

$$\text{rk}^M(I) := \text{rank}(\lim M|_I \rightarrow \text{colim} M|_I).$$

We refer the reader to MacLane (1971) for the definitions of limit, colimit, and the construction of the canonical limit-to-colimit map.

One of the very useful properties of generalized rank is that it is monotone w.r.t. the inclusion of posets. We use this property to define ZZ-GRIL.

Monotone Property of Generalized Rank. It follows from the definition that $\text{rk}^M(I) \leq \text{rk}^M(J)$ for all $J \subseteq I$, where I and J are subposets in P .

To exploit the topological features captured by generalized ranks, we use a cover of the quasi zigzag poset with a specific set of subposets called worms. When endowed with \mathbb{Z}^2 ordering, these subposets become $(3, 3)$ -intervals around a set of chosen *centers* with some chosen *widths*. Definition 3.1 gives precise definitions of these terms. We expand each of these worms, that is, increase the widths of these $(3, 3)$ -intervals while keeping the centers fixed. The monotonicity of the generalized rank ensures that it can only decrease or remain the same by this expansion. In Figure 1(right) a $(1, 1)$ -interval (rectangle) is expanded maximally to decrease the generalized rank from 3 to 1. The width for which the rank drops below a chosen threshold is taken as the ZZ-GRIL value at the center of the interval. Definition 3.2 makes this concept precise. The set of ZZ-GRIL values at the chosen centers makes a vector that we use in the learning pipeline.

3 ZZ-GRIL

In this section, we introduce concepts and definitions required for ZZ-GRIL. Then, we define ZZ-GRIL and discuss its theoretical properties. Keep in mind that, even if we do not explicitly state it always, these concepts apply to QZPH setting where vector spaces and linear maps in question are given by simplicial homology groups and homomorphisms between them induced by the input bi-filtrations.

Consider the poset $\mathbb{ZZ} \times \mathbb{Z}$ with the product order, i.e., $(\mathbf{z}_1, z_2) \leq (\mathbf{w}_1, w_2)$ if $\mathbf{z}_1 \leq \mathbf{w}_1$ in \mathbb{ZZ} and $z_2 \leq w_2$ in \mathbb{Z} . Note that $\mathbb{ZZ} \times \mathbb{Z}$ is equivalent to \mathbb{Z}^2 as sets. Thus, every subposet $P \subseteq \mathbb{ZZ} \times \mathbb{Z}$ can be thought as a subposet $P^{\mathbb{Z}^2} \subseteq \mathbb{Z}^2$ that is endowed with \mathbb{Z}^2 ordering. Interestingly, an interval in \mathbb{Z}^2 may not remain an interval in $\mathbb{ZZ} \times \mathbb{Z}$ and vice-versa.

We define a *quasi zigzag bi-filtration* over a quasi zigzag poset P as a collection of simplicial complexes $\{K_{\mathbf{p}}\}_{\mathbf{p} \in P}$, where $K_{\mathbf{p}} \subseteq K_{\mathbf{q}}$ for all comparable $\mathbf{p} \leq \mathbf{q}$. Akin to 1-parameter and zigzag persistence modules, inclusion-induced linear maps between the homology vector spaces of simplicial complexes in a quasi zigzag bi-filtration define a quasi zigzag persistence module.

We now define a special type of subposet in $\mathbb{ZZ} \times \mathbb{Z}$ which in \mathbb{Z}^2 is an ℓ -worm introduced by Xin et al. (2023) for $\ell = 2$.

Definition 3.1 (Worm). Let $\mathbf{p} \in \mathbb{ZZ} \times \mathbb{Z}$ and $\delta \in \mathbb{Z}$ be given. Let $\boxed{\mathbf{p}}_{\delta}$ denote the δ -square centered at \mathbf{p} , i.e., $\boxed{\mathbf{p}}_{\delta} := \{\mathbf{z} \in \mathbb{ZZ} \times \mathbb{Z} : \|\mathbf{p} - \mathbf{z}\|_{\infty} \leq \delta\}$. Then, a *worm* centered at \mathbf{p} with *width* δ is defined as the union of $\boxed{\mathbf{p}}_{\delta}$ with the two δ -squares $\boxed{\mathbf{q}}_{\delta}$ centered at points $\mathbf{q} = \mathbf{p} \pm (\delta, -\delta)$ on the off-diagonal line segment. We denote the worm as $\boxed{\mathbf{p}}_{\delta}^2$. The superscript denotes the number of δ -squares in the union apart from $\boxed{\mathbf{p}}_{\delta}$.

We note that computing $\|\cdot\|_{\infty}$ in $\mathbb{ZZ} \times \mathbb{Z}$ is equivalent to computing it in \mathbb{Z}^2 using the notion of set equivalence. We can see that a worm turns out to be a $(3, 3)$ -interval in \mathbb{Z}^2 . Refer to Figure 2 for an illustration of a worm.

Definition 3.2 (ZZ-GRIL). Let M be a quasi zigzag persistence module. Then, the *ZigZag Generalized Rank Invariant Landscape* is a function $\lambda^M : \mathbb{ZZ} \times \mathbb{Z} \times \mathbb{N} \rightarrow \mathbb{N}$ defined as

$$\lambda^M(\mathbf{p}, k) := \sup \left\{ \delta \geq 0 : \text{rk}^M \left(\boxed{\mathbf{p}}_{\delta}^2 \right) \geq k \right\},$$

where $\mathbf{p} \in \mathbb{ZZ} \times \mathbb{Z}$.

The basic idea of ZZ-GRIL is similar to GRIL. However, we note that the underlying poset structure is very different. We cover $\mathbb{ZZ} \times \mathbb{Z}$ with subposets of specific shapes (worms), and compute generalized rank over these worms to define the landscape function (ZZ-GRIL). Next, we show that ZZ-GRIL as an invariant remains stable.

3.1 Stability of ZZ-GRIL

We prove the stability of ZZ-GRIL by showing that its perturbation is bounded by the interleaving distance between two quasi zigzag persistence modules. The definition of interleaving distance (see Definition A.3 in Appendix A) between two zigzag persistence modules can be extended to quasi zigzag persistence modules.

There is an alternate notion of proximity on the space of persistence modules which uses Generalized Ranks computed on all intervals. This is known as *erosion distance* Kim & Mémoli (2021). We define a distance similar to erosion distance on the space of quasi zigzag persistence modules based on their generalized ranks computed over worms. For this, we need the notion of ϵ -thickening.

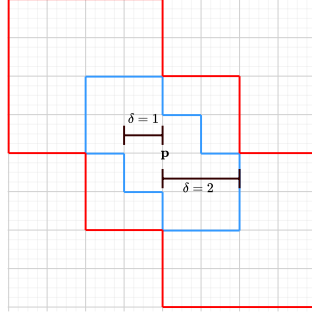


Figure 2: The worm with blue boundary represents a worm centered at \mathbf{p} with width $\delta = 1$. The worm with green boundary represents an expanded worm, centered at \mathbf{p} with width $\delta = 2$.

Let $\mathbf{I}(\mathbb{Z}\mathbb{Z} \times \mathbb{Z})$ denote the collection of all subposets in $\mathbb{Z}\mathbb{Z} \times \mathbb{Z}$ such that their corresponding subposets in \mathbb{Z}^2 are intervals. For $\epsilon \in \mathbb{Z}_+$, the ϵ -thickening of I is defined as

$$I^\epsilon := \{\mathbf{r} \in \mathbb{Z}\mathbb{Z} \times \mathbb{Z} : \exists \mathbf{q} \in I \text{ such that } \|\mathbf{r} - \mathbf{q}\|_\infty \leq \epsilon\}.$$

Definition 3.3. Let \mathcal{L} denote the collection of all worms in $\mathbb{Z}\mathbb{Z} \times \mathbb{Z}$. Let M and N be quasi zigzag persistence modules. The erosion distance is defined as:

$$d_{\mathcal{L}}^{\mathcal{L}}(M, N) := \inf_{\epsilon \geq 0} \{ \sqrt{\overline{\mathbf{p}}_\delta^2} \in \mathbf{I}(\mathbb{Z}\mathbb{Z} \times \mathbb{Z}), \\ \text{rk}^M(\overline{\mathbf{p}}_\delta^2) \geq \text{rk}^N(\overline{\mathbf{p}}_{\delta+\epsilon}^2) \text{ and} \\ \text{rk}^N(\overline{\mathbf{p}}_\delta^2) \geq \text{rk}^M(\overline{\mathbf{p}}_{\delta+\epsilon}^2) \}.$$

Note that $\overline{\mathbf{p}}_{\delta+\epsilon}^2$ contains the ϵ -thickening of $\overline{\mathbf{p}}_\delta^2$.

Proposition 3.4. Given two quasi zigzag persistence modules M and N , $d_{\mathcal{L}}^{\mathcal{L}}(M, N) \leq d_{\mathcal{I}}(M, N)$ where $d_{\mathcal{I}}$ denotes the interleaving distance between M and N .

Proposition 3.4 leads us to Theorem 3.5.

Theorem 3.5. Let M and N be two quasi zigzag persistence modules. Given appropriate \mathbf{p}, k , let the ZZ-GRIL of M and N over $\overline{\mathbf{p}}_\delta^2$ be λ^M and λ^N respectively. Then,

$$|\lambda^M(\mathbf{p}, k) - \lambda^N(\mathbf{p}, k)| = d_{\mathcal{L}}^{\mathcal{L}}(M, N) \leq d_{\mathcal{I}}(M, N).$$

Corollary 3.6 (Stability). Let M and N be two quasi zigzag persistence modules. Then,

$$\|\lambda^M - \lambda^N\|_\infty \leq d_{\mathcal{I}}(M, N).$$

We refer the reader to Appendix A for all the proofs.

4 Algorithm

We discuss the details of computing ZZ-GRIL in this section. We begin by proving that generalized rank over a subposet in $\mathbb{Z}\mathbb{Z} \times \mathbb{Z}$ can also be computed by computing the number of full bars in the zigzag filtration along the “boundary” of the subposet. To be precise, we introduce the following concepts now. Let P be any finite connected poset. We say a point $q \in P$ covers a point $p \in P$, denoted $p \prec q$ or $q \succ p$, if $p \leq q$ and there is no $r \in P$, $r \neq p, q$, so that $p \leq r \leq q$. A covering path $p \sim q$ between p and q is either a set of points $\{p = p_0 \prec p_1 \prec \dots \prec p_\ell = q\}$ or $\{p = p_0 \succ p_1 \succ \dots \succ p_\ell = q\}$. We define some special points in P . The set of minima in P are the points $P_{\min} = \{p \in P \mid \nexists r \neq p \in P \text{ where } r \leq p\}$. Similarly, define the set of maxima P_{\max} . For any two points $p, q \in P$, let $p \vee q$ and $p \wedge q$ denote their least upper bound (lub) and largest lower bound (llb) in P if they exist.

Now consider a subposet $I \subseteq \mathbb{Z}\mathbb{Z} \times \mathbb{Z}$ whose counterpart $I^{\mathbb{Z}^2}$ with \mathbb{Z}^2 ordering becomes an interval. Since $I^{\mathbb{Z}^2} \subset \mathbb{Z}^2$, its points can be sorted with increasing x -coordinates in \mathbb{Z}^2 . Let $I_{min}^{\mathbb{Z}^2} = \{p_0, \dots, p_s\}$ and $I_{max}^{\mathbb{Z}^2} = \{q_0, \dots, q_t\}$ be the set of minima and maxima respectively sorted according to their x -coordinates. The *lower fence* and *upper fence* of $I^{\mathbb{Z}^2}$ are defined as the paths

$$\begin{aligned} L_I^{\mathbb{Z}^2} &:= p_0 \sim (p_0 \vee p_1) \sim p_1 \sim (p_1 \vee p_2) \sim p_2 \sim \dots \sim p_s \\ U_I^{\mathbb{Z}^2} &:= q_0 \sim (q_0 \wedge q_1) \sim q_1 \sim (q_1 \wedge q_2) \sim q_2 \sim \dots \sim q_t. \end{aligned}$$

Consider the boundary $B_I^{\mathbb{Z}^2}$ comprising $L_I^{\mathbb{Z}^2}, U_I^{\mathbb{Z}^2}$, the paths $p_0 \sim q_0$ and $p_s \sim q_t$ going through the top left and bottom right corner points of $I^{\mathbb{Z}^2}$ respectively. Consider the subposet $I \subseteq \mathbb{Z}\mathbb{Z} \times \mathbb{Z}$ and observe that $I_{min}, I_{max} \subseteq B_I^{\mathbb{Z}^2}$ because all other points have one point below and another above in the y -direction. Let $\partial_L I, \partial_U I$, and ∂I be minimal paths in $B_I^{\mathbb{Z}^2}$ connecting all minima in I_{min} , all maxima in I_{max} , and all minima, maxima together respectively. Drawing an analogy to Dey et al. (2024) we call ∂I a *boundary cap* which is drawn orange in Figure 3.

Next, we appeal to certain results in category theory to claim a result analogous to Dey et al. (2024) that helps computing the generalized ranks with zigzag persistence modules. Treating I as a category with points in I as objects and relations as morphisms, we get $\partial_L I$ and $\partial_U I$ as subcategories. Then, we get functors $F_L : \partial_L I \rightarrow I$ induced by inclusion and $F_U : I \rightarrow \partial_U I$ induced by projection which have some special properties.

Definition 4.1. A connected subposet $P' \subseteq P$ is called *initial* if for every $p \in P \setminus P'$, the downset $\downarrow p = \{q \in P \mid q \neq p \ \& \ q \leq p\}$ intersects P' in a connected poset. Similarly, P' is called *terminal* if for every $p \in P \setminus P'$, the upset $\uparrow p = \{q \in P \mid q \neq p \ \& \ q \geq p\}$ intersects P' in a connected poset.

We call a functor $F : P' \rightarrow P$ for $P' \subseteq P$ *initial* if P' is initial. Similarly, we call $F : P \rightarrow P'$ *terminal* if P' is terminal. The following result connecting initial (terminal) functor to the limit (colimit) is well known, [Chapter 8] Riehl (1914).

Proposition 4.2. Let $M : P \rightarrow \mathbf{vec}$ be a persistence module and $F_L : P' \rightarrow P$ and $F_U : P \rightarrow P''$ be initial and terminal functors. Then, there is an isomorphism $\phi : \lim M \rightarrow \lim M|_{P'}$ from the limit of M to the limit of the restricted module $M|_{P'}$. Similarly, we have an isomorphism for colimits, $\psi : \text{colim } M|_{P''} \rightarrow \text{colim } M$.

We observe that the functors $F_L : \partial_L I \rightarrow I$ and $F_U : I \rightarrow \partial_U I$ mentioned earlier are initial and terminal respectively allowing us to use Proposition 4.2.

Proposition 4.3. $F_L : \partial_L I \rightarrow I$ is an initial functor and $F_U : I \rightarrow \partial_U I$ is a terminal functor.

Proof. It is sufficient to prove that $\partial_L I$ is initial for F_L and $\partial_U I$ is terminal for F_U . We only show that $\partial_L I$ is initial and the proof for $\partial_U I$ being terminal is similar.

Let $p \in I \setminus \partial_L I$ be any point. Let p^- and p^+ be two points (if exist) where $p^- \prec p$ and $p^+ \succ p$ in \mathbb{Z}^2 with $p_x^- < p_x < p_x^+$. By definition of the quasi zigzag poset, either $p^- \succ p$ and $p^+ \succ p$, or $p^- \prec p$ and $p^+ \prec p$ in the poset $\mathbb{Z}\mathbb{Z} \times \mathbb{Z}$.

In the first case, the downset $\downarrow p$ consists of all points $p' \neq p$ that are vertically below p , that is, $p'_x = p_x$ and $p'_y < p_y$. This means $\downarrow p$ intersects $\partial_L I$ in a connected poset $p'_0 < \dots < p'_k$ where each p'_i has the same x -coordinate as p .

In the second case, the downset $\downarrow p$ consists of three sets of points Y^{p^-}, Y^p , and Y^{p^+} that are vertically below p^-, p , and p^+ respectively. Each of Y^{p^-}, Y^p and Y^{p^+} intersects $\partial_L I$ in a connected poset. They can be disconnected as a whole only if there is a point $q \in \partial_L I$ so that $p_x^- < q_x < p_x$ or $p_x < q_x < p_x^+$. But, neither is possible because p^- and p^+ are points in I covered by p . \square

Following proposition is immediate.

Proposition 4.4. $\partial(\partial_L I) = \partial_L I$ and $\partial(\partial_U I) = \partial_U I$.

Now, we prove the following result which extends Theorem 3.1 in Dey et al. (2024) from 2-parameter persistence modules to the quasi zigzag persistence modules.

Theorem 4.5. Let $M : P \rightarrow \mathbf{vec}$ be a quasi zigzag persistence module and $I \subseteq P$ be a finite subposet so that $I^{\mathbb{Z}^2}$ is an interval. Then, $\text{rk}^M(I) = \text{rk}^M(\partial I)$.

Proof. Let r denote the map $r : \lim I \rightarrow \text{colim } I$, and $\phi : \lim I \rightarrow \lim \partial_L I$ and $\psi : \text{colim } \partial_U I \rightarrow \text{colim } I$ be the isomorphisms guaranteed by Proposition 4.2. Observe that $\text{rk}^M(I) = \text{rank}(\psi^{-1} \circ r \circ \phi^{-1})$. Now let r' denote the

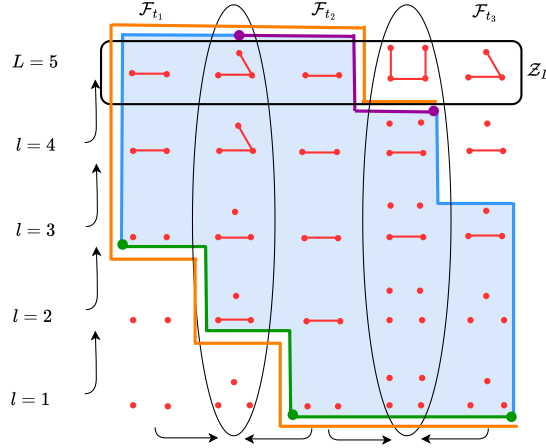


Figure 3: A worm I (shaded) on a quasi zigzag bi-filtration where the direction of the inclusion on horizontal arrows are shown at the bottom and on the vertical arrows on left. The worm centered at $(3,3)$ has width 1. The part of the boundary colored green is $\partial_L I$ connecting the minima shown as green points and the part in purple is $\partial_U I$ connecting the maxima shown as purple points. The *boundary cap* is shown in orange which runs parallel to the boundary for a portion of it. Refer to Figure 5 for the zigzag filtration along the boundary cap of the worm. A sequence of graphs with $T = 3$ time steps is shown with the corresponding graph filtrations: $\mathcal{F}_{t_1}, \mathcal{F}_{t_2}, \mathcal{F}_{t_3}$ each with $L = 5$ levels. The filtration of the unions are encircled by ovals. Zigzag filtration at the topmost level \mathcal{Z}_L is shown in a rectangular box.

map $r' : \lim \partial I \rightarrow \text{colim} \partial I$. Consider the isomorphisms $\phi' : \lim \partial I \rightarrow \lim \partial(\partial_L I)$ and $\psi' : \text{colim} \partial(\partial_U I) \rightarrow \text{colim} \partial I$ again guaranteed by Proposition 4.2. Then, $\text{rk}^M(\partial I) = \text{rank}(\psi'^{-1} \circ r' \circ \phi'^{-1})$. But, $\psi'^{-1} \circ r' \circ \phi'^{-1} = \psi'^{-1} \circ r' \circ \phi'^{-1}$ because of Proposition 4.4. \square

With this background, the pipeline for computing ZZ-GRIL in the QZPH framework can be described as follows. Suppose that we are given sequential data (sequence of point clouds, sequence of graphs, multivariate time series) with vertex-level correspondences between consecutive time steps. First, we build a quasi zigzag bi-filtration out of this data where time increases in x -direction and the threshold for constructing complexes increases in y -direction. The algorithm for building this bi-filtration out of raw data is described in section 4.1 where we make certain choices to make it efficient. Each simplicial complex in the bi-filtration is indexed by a finite grid G in \mathbb{Z}^2 because $\mathbb{Z}\mathbb{Z} \times \mathbb{Z}$ is equivalent to \mathbb{Z}^2 as sets. We sample a set of center points S from G and compute ZZ-GRIL (Definition 3.2) at each of these center points. Taking advantage of Theorem 4.5, we compute ZZ-GRIL by computing the zigzag filtration along the boundary cap (a path) of a worm centering each point in S and then computing the number of full bars in the corresponding zigzag persistence module obtained by applying the homology functor.

A sequence of point clouds (Figure 1) or graphs (Figure 3) or multivariate time-series data (refer section 5 for converting multivariate time-series to a sequence of point clouds or graphs) gives us a collection of simplicial complexes. Every simplex in each simplicial complex is assigned a weight which is derived from the input. We build a quasi zigzag bi-filtration from this collection of simplicial complexes.

4.1 Building Quasi Zigzag Bi-filtration

We explain the algorithm by considering an example of sequential graph data, as shown in Figure 4. We assume that each graph has edge-weights. In the top row of Figure 4, notice that the first two graphs can not be linked by an inclusion in any direction, i.e., neither is a subgraph of the other. This is because, there is an inclusion of an edge (v_2, v_3) as well as a deletion (v_1, v_4) . We circumvent this problem by clubbing all inclusions together followed by all deletions. This is equivalent to considering the union of the two graphs as the intermediary step and then deleting the edges which are not present in the previous graph. Refer to the bottom row of Figure 4, where the intermediary union graphs are shown along with the original graphs.

A sequence of T number of graphs is converted into a zigzag filtration \mathcal{Z}_L of length $2T - 1$ by the above procedure because every consecutive pair of graphs introduces a union in between. For each graph in the zigzag filtration thus

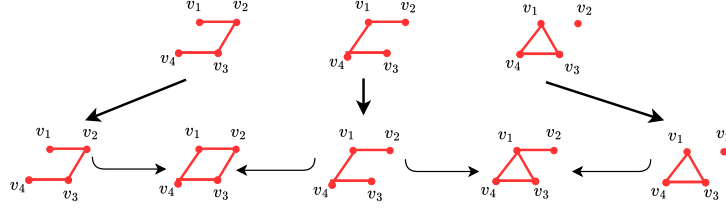


Figure 4: The top row shows a typical input to the ZZ-GRIL framework as a sequence of graphs. This sequence has 3 graphs. Observe that consecutive graphs cannot be linked by an inclusion in either direction because neither is a subgraph of the other. In order to circumvent this problem, we consider the unions of consecutive graphs as an intermediary step, as shown in the bottom row.

obtained, we construct its *graph filtration* based on edge-weights; see e.g. Dey & Wang (2022); Edelsbrunner & Harer (2010). We ensure that the length of each graph filtration remains the same by considering the sublevel sets of exactly L levels. The zigzag filtration at the highest level, \mathcal{Z}_L , can be pulled back to each lower level l . This ensures that we get a zigzag filtration \mathcal{Z}_l at each level $1 \leq l < L$ of the filtration. This gives us a quasi zigzag bi-filtration. Refer to Figure 3 for an illustration of a quasi zigzag bi-filtration.

While implementing this procedure, we need not compute the union graphs explicitly saving both storage and time because all necessary information is already present in the corresponding component graphs. We use the following procedure to efficiently build the quasi zigzag bi-filtration.

Construct the graph filtration \mathcal{F}_{t_i} of each of the T graphs in the sequential graph data, where $1 \leq t_i \leq T$. Let σ be a simplex that is inserted at the level l in the filtration \mathcal{F}_{t_i} . We have three possible scenarios for σ in $\mathcal{F}_{t_{i+1}}$:

1. σ is inserted in $\mathcal{F}_{t_{i+1}}$ at m for some $m < l$: In this case, σ needs to be added on all the horizontal inclusion arrows $K_{t_i,w} \hookrightarrow K_{t_i,w} \cup K_{t_{i+1},w}$ for $m \leq w < l$.
2. σ is inserted in $\mathcal{F}_{t_{i+1}}$ at m for some $m \geq l$: In this case, σ needs to be added on all the horizontal inclusion arrows $K_{t_{i+1},w} \hookrightarrow K_{t_i,w} \cup K_{t_{i+1},w}$ for $l \leq w < m$.
3. σ is not present in $\mathcal{F}_{t_{i+1}}$. In this case, we treat it as getting inserted at the maximum level L in $\mathcal{F}_{t_{i+1}}$ and hence, will be added by the inclusion $K_{t_{i+1},L} \hookrightarrow K_{t_i,L} \cup K_{t_{i+1},L}$.

We repeat this procedure for the pair \mathcal{F}_{t_i} and $\mathcal{F}_{t_{i-1}}$.

Since we are working with an integer grid, we can simulate the quasi zigzag bi-filtration such that we have the standard filtration \mathcal{F}_{t_i} at even x -coordinates and at odd x -coordinates, we have the standard filtration of the unions, without explicitly storing the unions.

Correctness. To prove the correctness of the procedure, we need to show the following: For $1 \leq i, i' \leq T$ and $1 \leq j, j' \leq L$, let $K_{i,j}$ denote the simplicial complex in the quasi zigzag filtration built according to the procedure mentioned above and $K'_{i,j}$ is the simplicial complex in the quasi zigzag bi-filtration built by considering unions explicitly. We show that the new simplices inserted by the inclusion $K_{i,j} \hookrightarrow K_{i',j'}$ are the same as the ones inserted by $K'_{i,j} \hookrightarrow K'_{i',j'}$.

Proof. The statement is immediately true for the inclusions $i' = i, j' = j + 1$. This is because the new simplices in the upward (y -direction) inclusions are the ones born at the level $j + 1$ in the input family of filtrations. Now, we prove the statement for the case where $i' = i \pm 1, j' = j$, i.e., the horizontal (x -direction) inclusions/deletions. Note that we have inclusions from $K_{i,j} \hookrightarrow K_{i',j'}$ only when i is an even integer and $i' = i \pm 1$. We prove it for the case $i' = i + 1, j' = j$. The proof for the other case is similar. Let σ be a simplex added on the inclusion $K_{i,j} \hookrightarrow K_{i+1,j}$. According to the procedure described above, it means that σ is born at some level $j_1 \leq j$ in the filtration \mathcal{F}_{i+2} and is not born before level j in the filtration \mathcal{F}_i . Hence, σ will be newly added on the arrow $K'_{i,j} \hookrightarrow K'_{i+1,j}$ because $\sigma \in K'_{i+2,j}$ and $\sigma \notin K'_{i,j}$. This is because $K_{i,j} = K'_{i,j}$ for all even integers i , as they are the simplicial complexes part of the input filtrations \mathcal{F}_i . By the same arguments, all the newly added simplices on inclusions $K'_{i,j} \hookrightarrow K'_{i+1,j}$ will be newly added simplices on $K_{i,j} \hookrightarrow K_{i+1,j}$. \square

Methods	Accuracy	F-1 Overall	F-1 Wake	F-1 N-1	F-1 N2	F-1 N3	F-1 REM
SVM Alickovic & Subasi (2018)	73.3	72.1	86.8	52.3	69.9	78.6	73.1
RF Memar & Faradji (2017)	72.9	70.8	85.8	47.3	70.4	80.9	69.9
MLP+LSTM Dong et al. (2017)	77.9	75.8	86.0	46.9	76.0	87.5	82.8
CNN+BiLSTM Supratak et al. (2017)	78.8	77.9	88.7	60.2	74.6	85.8	80.2
CNN Chambon et al. (2018)	78.1	76.8	87.0	55.0	76.0	85.1	80.9
ARNN+RNN Phan et al. (2019)	78.9	76.3	83.6	43.9	79.3	87.9	86.7
STGCN Jia et al. (2020)	79.9	78.7	87.8	57.4	77.6	86.4	84.1
MSTGCN Jia et al. (2021)	82.1	80.8	89.4	59.6	80.6	89.0	85.6
STDP-GCN Zhao et al. (2023)	82.6	81.0	83.5	62.9	83.1	86.0	90.6
STDP-GCN + ZZ-GRIL	83.8	81.1	88.6	58.1	85.4	82.7	90.9

Table 1: Accuracy and F-1 scores of augmenting ZZ-GRIL to STDP-GCN and testing on ISRUC-S3 sleep classification dataset. We report the overall accuracy, the overall F-1 score and sleep-stage-wise F-1 scores for each model.

Dataset/Methods	ED-1NN	DTW-1NN-I	DTW-1NN-D	MLSTM-FCN	ShapeNet	WEASEL+MUSE	TapNet	OS-CNN	MOS-CNN	TodyNet	TodyNet+ZZ-GRIL
FingerMovements	0.550	0.520	0.530	0.580	0.589	0.490	0.530	0.568	0.568	0.570	0.660
Heartbeat	0.620	0.659	0.717	0.663	0.756	0.727	0.751	0.489	0.604	0.756	0.756
MotorImagery	0.510	0.390	0.500	0.510	0.610	0.500	0.590	0.535	0.515	0.640	0.660
NATOPS	0.860	0.850	0.883	0.889	0.883	0.870	0.939	0.968	0.951	0.972	0.961
SelfRegulationSCP2	0.483	0.533	0.539	0.472	0.578	0.460	0.550	0.532	0.510	0.550	0.600

Table 2: Accuracy of augmenting ZZ-GRIL to TodyNet and testing on UEA Multivariate Time Series Classification Datasets.

the machine learning model which has the highest performance to truly test and highlight the value of the topological information added by ZZ-GRIL to an already high-performing specifically tailored model.

5.1 Experimental Setup

Each data instance is a multivariate time-series. We convert multivariate time-series data into a quasi zigzag bi-filtration. The ZZ-GRIL framework takes in a quasi zigzag bi-filtration as input and provides a topological signature for the sequence as output. We augment the machine learning model with this topological information and train the model for classification. The framework is shown in Figure 6.

Given a sample of multivariate time-series data with m time-series, we splice each time-series into a *sequence of time-series*, each of length w . This splicing is done by a moving window of width w , where consecutive windows have an overlap of λ . We calculate the Pearson correlation coefficient Pearson & Lee (1903) between time-series in each window. We construct a graph for each window, where each time-series (of length w) is a node, and edges with the Pearson correlation values as weights connect them. Thus, we get a complete graph with m nodes. We select the top k percentile of these edges to build the final graph in each window. This way we obtain a sequence of graphs. The topological information of this sequence of graphs encodes the evolution of correlation between time series. Alternately, we can also track the evolving time-series by converting it into a sequence of point clouds. From the sequence of time-series described above, we consider each time-series of length w as a point in \mathbb{R}^w . Thus, if we have m time series, we have m points in \mathbb{R}^w in each window. Thus, we get a sequence of point clouds in \mathbb{R}^w . This sequence of point clouds tracks the evolution of each time-series, and a Vietoris-Rips like construction on this point cloud tracks the evolution of the interaction between time-series. Refer to Figure 6 for an illustration. Refer to Appendix B for hyperparameters.

5.2 UEA Multivariate Time Series Classification

UEA Multivariate Time Series Classification (MTSC) Bagnall et al. (2018) archive comprises of real-world multivariate time series data and is a widely recognized benchmark in time series analysis. The UEA MTSC collection encompasses a diverse range of application domains such as healthcare (ECG or EEG data), motion recognition (recorded using wearable sensors). See Table 5 in Appendix B.

The datasets are preprocessed and split into training and testing sets. We use these train-test splits and compare the performance, by augmenting ZZ-GRIL to TodyNet, Liu et al. (2024) with existing methods Li et al. (2021); Tang et al. (2022); Karim et al. (2019); Schäfer & Leser (2017). For this set of experiments, we convert the multivariate time series into a sequence of point clouds and compute ZZ-GRIL. We choose 5 datasets which have at least 7 multivariate time series. This ensures that each point cloud, in the sequence of point clouds, has at least 7 points, giving meaningful topological information. Refer to Figure 7 for a visualization of ZZ-GRIL on FingerMovements dataset processed

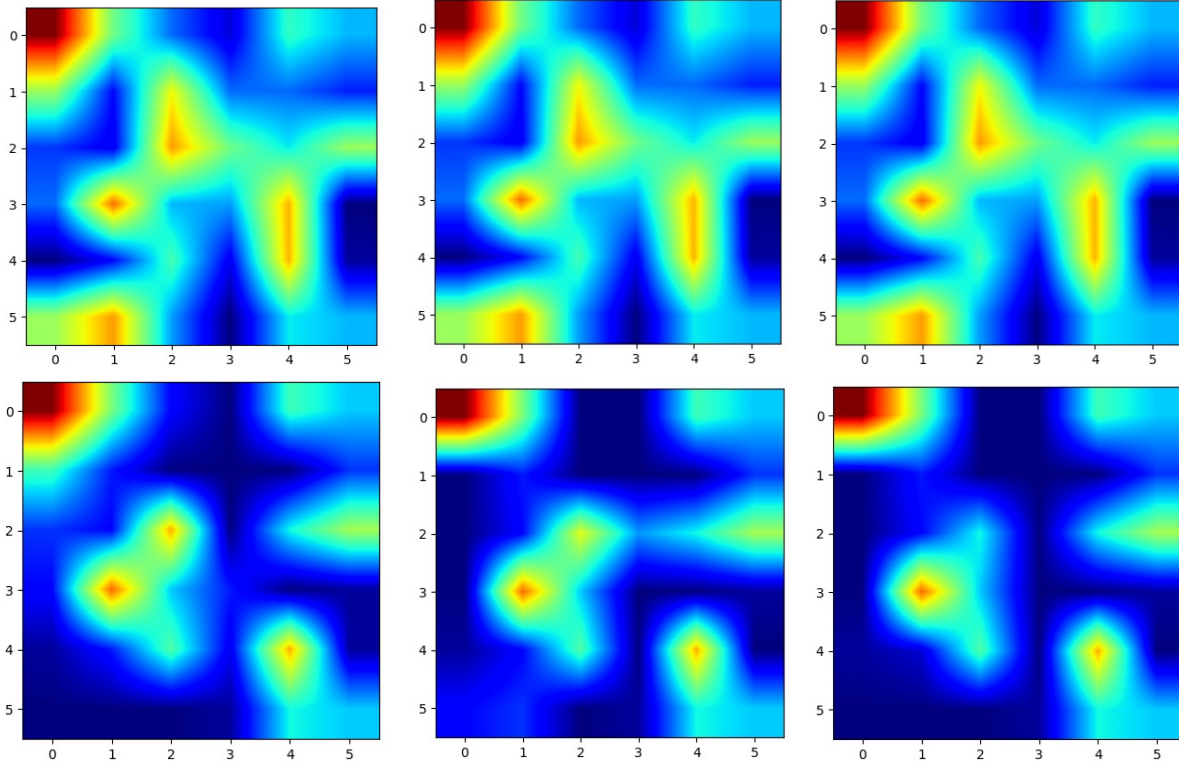


Figure 7: Heatmap of ZZ-GRIL on the FingerMovements dataset. ZZ-GRIL is computed at 36 center points, which is plotted as a 6x6 grid. The top row represents three samples with label 1 and the bottom row represents three samples with label 0. We can see the similarity in the ZZ-GRIL signatures between samples of the same class and clear differences between samples of different classes.

Dataset	Time (ZZ-GRIL point clouds)	Time (ZZ-GRIL graphs)
FingerMovements	569s	138s
NATOPS	413s	68s
SelfRegulationSCP2	153s	27s

Table 3: Computation times for ZZ-GRIL. The values represent the computation times for both training and testing splits. All the experiments were performed on Intel(R) Xeon(R) Gold 6248R CPU and NVIDIA Quattro RTX 6000 GPU.

as a sequence of point clouds. We report the results in Table 2. We can see that augmenting ZZ-GRIL improves the performance in most cases.

We perform another set of experiments where we compare the performance of converting the multivariate time series into sequence of point clouds versus converting it into sequence of graphs for extracting topological information. We report the results in Table 4. We can see that both of these approaches are viable choices.

Dataset	TodyNet + ZZ-GRIL point clouds	TodyNet + ZZ-GRIL graphs
FingerMovements	0.660	0.680
NATOPS	0.961	0.945
SelfRegulationSCP2	0.600	0.594

Table 4: Comparison of converting multivariate time series as a sequence of point clouds versus converting it as a sequence of graphs to extract the topological information.

5.3 Sleep Stage Classification

We use ISRUC-S3 dataset, which is a part of the ISRUC (Iberian Studies and Research on Sleep) Sleep Dataset Khalighi et al. (2016). ISRUC-S3 contains PSG recordings from 10 subjects. Each recording includes multiple physiological signals, such as: EEG, ECG. The dataset is annotated with sleep stage labels for each epoch (30 second window). There are 5 sleep stage labels: Wake (W), N1, N2, N3 (non-REM stages) and REM. We use STDP-GCN Zhao et al. (2023) as the machine learning model to augment. In this experiment, we convert the time series into sequence of graphs and compare the performance in Table 1. We can see that augmenting ZZ-GRIL increases both the accuracy and the overall F-1 score.

We would like to clarify that the aim, for both sets of experiments, is primarily to show that an increase in accuracy signifies that ZZ-GRIL captures meaningful topological information which can be used to improve the existing models.

We report the computation times in Table 3. We can see from the table that ZZ-GRIL is, indeed, practical to use.

6 Conclusion

In this paper, we proposed QZPH as a framework to capture both static and dynamic topological features in time-varying data. We proposed ZZ-GRIL, a stable and computationally efficient topological invariant to address the challenges of integrating MPH and ZPH. Through applications in various domains, including sleep-stage detection, we showed that augmenting machine learning models with ZZ-GRIL improves the performance. These results highlight the potential of integrating topological information to address complex challenges while analyzing time-evolving data. The differentiability of ZZ-GRIL is an interesting research avenue. Further, it would also be interesting to study how other multiparameter methods adapt to the QZPH framework.

7 Acknowledgement

This work is partially supported by NSF grants DMS-2301360 and CCF-2437030. We acknowledge the discussion with Michael Lesnick who pointed out the theory about initial/terminal functors in the context of limits and colimits.

References

- Alickovic, E. and Subasi, A. Ensemble SVM method for automatic sleep stage classification. *IEEE Transactions on Instrumentation and Measurement*, 67(6):1258–1265, 2018. URL <https://ieeexplore.ieee.org/document/8292946>.
- Bagnall, A., Dau, H. A., Lines, J., Flynn, M., Large, J., Bostrom, A., Southam, P., and Keogh, E. The UEA multivariate time series classification archive, 2018, 2018. URL <https://arxiv.org/abs/1811.00075>.
- Botnan, M. and Lesnick, M. Algebraic stability of zigzag persistence modules. *Algebraic & geometric topology*, 18(6): 3133–3204, 2018. URL <https://msp.org/agt/2018/18-6/agt-v18-n6-p01-s.pdf>.
- Bouritsas, G., Frasca, F., Zafeiriou, S. P., and Bronstein, M. Improving graph neural network expressivity via subgraph isomorphism counting. *IEEE Transactions on Pattern Analysis and Machine Intelligence*, pp. 1–1, 2022. doi: 10.1109/TPAMI.2022.3154319. URL <https://doi.org/10.1109/TPAMI.2022.3154319>.
- Box, G. and Jenkins, G. M. *Time Series Analysis: Forecasting and Control*. Holden-Day, 1976.
- Bubenik, P. Statistical topological data analysis using persistence landscapes. *J. Mach. Learn. Res.*, 16:77–102, 2015. doi: 10.5555/2789272.2789275. URL <https://dl.acm.org/doi/10.5555/2789272.2789275>.
- Cang, Z. and Wei, G.-W. Topologynet: Topology based deep convolutional and multi-task neural networks for biomolecular property predictions. *PLOS Computational Biology*, 13(7):1–27, 07 2017. doi: 10.1371/journal.pcbi.1005690. URL <https://doi.org/10.1371/journal.pcbi.1005690>.
- Carrière, M. and Blumberg, A. Multiparameter persistence image for topological machine learning. In Larochele, H., Ranzato, M., Hadsell, R., Balcan, M., and Lin, H. (eds.), *Advances in Neural Information Processing Systems*, volume 33, pp. 22432–22444. Curran Associates, Inc., 2020. URL <https://proceedings.neurips.cc/paper/2020/file/fdff71fcab656abfbefabecab1a7f6d-Paper.pdf>.
- Carrière, M., Chazal, F., Ike, Y., Lacombe, T., Royer, M., and Umeda, Y. PersLay: A neural network layer for persistence diagrams and new graph topological signatures. In Chiappa, S. and Calandra, R. (eds.), *Proceedings of the Twenty Third International Conference on Artificial Intelligence and Statistics*, volume 108 of *Proceedings of Machine Learning Research*, pp. 2786–2796. PMLR, 26–28 Aug 2020. URL <https://proceedings.mlr.press/v108/carriere20a.html>.
- Chambon, S., Galtier, M. N., Arnal, P. J., Wainrib, G., and Gramfort, A. A deep learning architecture for temporal sleep stage classification using multivariate and multimodal time series. *IEEE Transactions on Neural Systems and Rehabilitation Engineering*, 26(4):758–769, 2018. URL <https://ieeexplore.ieee.org/document/8307462>.
- Chazal, F., Cohen-Steiner, D., Glisse, M., Guibas, L. J., and Oudot, S. Proximity of persistence modules and their diagrams. In Hershberger, J. and Fogel, E. (eds.), *Proceedings of the 25th ACM Symposium on Computational Geometry, Aarhus, Denmark, June 8-10, 2009*, pp. 237–246. ACM, 2009. doi: 10.1145/1542362.1542407. URL <https://doi.org/10.1145/1542362.1542407>.
- Chen, C., Ni, X., Bai, Q., and Wang, Y. A topological regularizer for classifiers via persistent homology. In *The 22nd International Conference on Artificial Intelligence and Statistics*, pp. 2573–2582. PMLR, 2019. URL <https://proceedings.mlr.press/v89/chen19g.html>.
- Chen, Y., Segovia, I., and Gel, Y. R. Z-GCNETs: Time zigzags at graph convolutional networks for time series forecasting. In *International Conference on Machine Learning*, pp. 1684–1694. PMLR, 2021. URL <https://proceedings.mlr.press/v139/chen21o/chen21o.pdf>.
- Chu, P., Wang, J., You, Q., Ling, H., and Liu, Z. Transmot: Spatial-temporal graph transformer for multiple object tracking. In *Proceedings of the IEEE/CVF Winter Conference on applications of computer vision*, pp. 4870–4880, 2023. URL https://openaccess.thecvf.com/content/WACV2023/papers/Chu_TransMOT_Spatial-Temporal_Graph_Transformer_for_Multiple_Object_Tracking_WACV_2023_paper.pdf.
- Corbet, R., Fugacci, U., Kerber, M., Landi, C., and Wang, B. A kernel for multi-parameter persistent homology. *Computers & Graphics: X*, 2:100005, 2019. ISSN 2590-1486. doi: <https://doi.org/10.1016/j.cagx.2019.100005>. URL <https://www.sciencedirect.com/science/article/pii/S2590148619300056>.
- Dey, T. K. and Hou, T. Fast Computation of Zigzag Persistence. In Chechik, S., Navarro, G., Rotenberg, E., and Herman, G. (eds.), *30th Annual European Symposium on Algorithms (ESA 2022)*, volume 244 of *Leibniz International Proceedings in Informatics (LIPIcs)*, pp. 43:1–43:15. Dagstuhl, Germany, 2022. Schloss Dagstuhl – Leibniz-Zentrum für Informatik. ISBN 978-3-95977-247-1. doi: 10.4230/LIPIcs.ESA.2022.43. URL <https://drops.dagstuhl.de/entities/document/10.4230/LIPIcs.ESA.2022.43>.
- Dey, T. K. and Wang, Y. *Computational Topology for Data Analysis*. Cambridge University Press, 2022. doi: 10.1017/9781009099950. URL <https://www.cs.purdue.edu/homes/tamaldey/book/CTDAbook/CTDAbook.pdf>.

- Dey, T. K., Kim, W., and Mémoli, F. Computing generalized rank invariant for 2-parameter persistence modules via zigzag persistence and its applications. *Discret. Comput. Geom.*, 71(1):67–94, 2024. doi: 10.1007/S00454-023-00584-Z. URL <https://doi.org/10.1007/s00454-023-00584-z>.
- Dong, H., Supratak, A., Pan, W., Wu, C., Matthews, P. M., and Guo, Y. Mixed neural network approach for temporal sleep stage classification. *IEEE Transactions on Neural Systems and Rehabilitation Engineering*, 26(2):324–333, 2017. URL <https://ieeexplore.ieee.org/document/7995122>.
- Edelsbrunner, H. and Harer, J. *Computational Topology: An Introduction*. Applied Mathematics. American Mathematical Society, 2010. ISBN 9780821849255.
- Fan, H., Yu, X., Ding, Y., Yang, Y., and Kankanhalli, M. PSTNet: Point spatio-temporal convolution on point cloud sequences. In *International Conference on Learning Representations*, 2021. URL https://openreview.net/forum?id=03bqkf_Puys.
- Flammer, M. and Hüper, K. Spatiotemporal persistence landscapes, 2024. URL <https://arxiv.org/abs/2412.11925>.
- Gabrielsson, R. B., Nelson, B. J., Dwaraknath, A., and Skraba, P. A topology layer for machine learning. In *The 23rd International Conference on Artificial Intelligence and Statistics, AISTATS 2020, 26-28 August 2020, Online [Palermo, Sicily, Italy]*, volume 108 of *Proceedings of Machine Learning Research*, pp. 1553–1563. PMLR, 2020. URL <http://proceedings.mlr.press/v108/gabrielsson20a.html>.
- Hamilton, J. D. *Time Series Analysis*. Princeton University Press, 1994. URL https://www.worldcat.org/title/time-series-analysis/oclc/1194970663&referer=brief_results.
- Hofer, C. D., Graf, F., Rieck, B., Niethammer, M., and Kwitt, R. Graph filtration learning. In *Proceedings of the 37th International Conference on Machine Learning, ICML 2020, 13-18 July 2020, Virtual Event*, volume 119 of *Proceedings of Machine Learning Research*, pp. 4314–4323. PMLR, 2020. URL <http://proceedings.mlr.press/v119/hofer20b.html>.
- Horn, M., Brouwer, E. D., Moor, M., Moreau, Y., Rieck, B., and Borgwardt, K. M. Topological graph neural networks. In *The Tenth International Conference on Learning Representations, ICLR 2022, Virtual Event, April 25-29, 2022*. OpenReview.net, 2022. URL <https://openreview.net/forum?id=oxxUMeFwEHd>.
- Huang, S., Xie, Y., Zhu, S.-C., and Zhu, Y. Spatio-temporal self-supervised representation learning for 3d point clouds. In *Proceedings of the IEEE/CVF International Conference on Computer Vision*, pp. 6535–6545, 2021. URL https://openaccess.thecvf.com/content/ICCV2021/papers/Huang_Spatio-Temporal_Self-Supervised_Representation_Learning_for_3D_Point_Clouds_ICCV_2021_paper.pdf.
- Jia, Z., Lin, Y., Wang, J., Zhou, R., Ning, X., He, Y., and Zhao, Y. GraphSleepNet: Adaptive spatial-temporal graph convolutional networks for sleep stage classification. In *Ijcai*, volume 2021, pp. 1324–1330, 2020. URL <https://www.ijcai.org/proceedings/2020/0184.pdf>.
- Jia, Z., Lin, Y., Wang, J., Ning, X., He, Y., Zhou, R., Zhou, Y., and Li-wei, H. L. Multi-view spatial-temporal graph convolutional networks with domain generalization for sleep stage classification. *IEEE Transactions on Neural Systems and Rehabilitation Engineering*, 29:1977–1986, 2021. URL <https://ieeexplore.ieee.org/abstract/document/9530406>.
- Kan, J., Hu, K., Hagenbuchner, M., Tsoi, A. C., Bennamoun, M., and Wang, Z. Sign language translation with hierarchical spatio-temporal graph neural network. In *Proceedings of the IEEE/CVF winter conference on applications of computer vision*, pp. 3367–3376, 2022. URL https://openaccess.thecvf.com/content/WACV2022/papers/Kan_Sign_Language_Translation_With_Hierarchical_Spatio-Temporal_Graph_Neural_Network_WACV_2022_paper.pdf.
- Karim, F., Majumdar, S., Darabi, H., and Harford, S. Multivariate LSTM-FCNs for time series classification. *Neural networks*, 116:237–245, 2019. URL https://www.sciencedirect.com/science/article/pii/S0893608019301200?casa_token=PDVs4qbGRbIAAAAA:zy34UVvHn2z55zyu_P3u1ILMj8TQBxrTt0LrBAQiVh_aVks7unsEXFEqnq2ywsCkcVDLrvI1Q.
- Khalighi, S., Sousa, T., Santos, J. M., and Nunes, U. ISRUC-Sleep: A comprehensive public dataset for sleep researchers. *Computer Methods and Programs in Biomedicine*, 124:180–192, 2016. ISSN 0169-2607. doi: <https://doi.org/10.1016/j.cmpb.2015.10.013>. URL <https://www.sciencedirect.com/science/article/pii/S0169260715002734>.
- Kim, K., Kim, J., Zaheer, M., Kim, J., Chazal, F., and Wasserman, L. PLLay: Efficient topological layer based on persistent landscapes. In Larochelle, H., Ranzato, M., Hadsell, R., Balcan, M., and Lin, H. (eds.), *Advances in Neural Information Processing Systems*, volume 33, pp. 15965–15977. Curran Associates, Inc., 2020. URL <https://proceedings.neurips.cc/paper/2020/file/b803a9254688e259cde2ec0361c8abe4-Paper.pdf>.

- Kim, W. and Mémoli, F. Generalized persistence diagrams for persistence modules over posets. *Journal of Applied and Computational Topology*, 5(4):533–581, 12 2021. ISSN 2367-1734. doi: 10.1007/s41468-021-00075-1. URL <https://doi.org/10.1007/s41468-021-00075-1>.
- Lesnick, M. and Wright, M. Interactive visualization of 2-d persistence modules. *CoRR*, abs/1512.00180, 2015. URL <http://arxiv.org/abs/1512.00180>.
- Li, G., Choi, B., Xu, J., Bhowmick, S. S., Chun, K.-P., and Wong, G. L.-H. Shapenet: A shapelet-neural network approach for multivariate time series classification. In *Proceedings of the AAAI conference on artificial intelligence*, volume 35, pp. 8375–8383, 2021.
- Liu, H., Yang, D., Liu, X., Chen, X., Liang, Z., Wang, H., Cui, Y., and Gu, J. TodyNet: Temporal dynamic graph neural network for multivariate time series classification. *Information Sciences*, 677:120914, 2024. ISSN 0020-0255. doi: <https://doi.org/10.1016/j.ins.2024.120914>. URL <https://www.sciencedirect.com/science/article/pii/S0020025524008284>.
- Liu, X., Yan, M., and Bohg, J. MeteorNet: Deep learning on dynamic 3d point cloud sequences. In *Proceedings of the IEEE/CVF International Conference on Computer Vision*, pp. 9246–9255, 2019. URL https://openaccess.thecvf.com/content_ICCV_2019/papers/Liu_MeteorNet_Deep_Learning_on_Dynamic_3D_Point_Cloud_Sequences_ICCV_2019_paper.pdf.
- Liu, X., Feng, H., Wu, J., and Xia, K. Dowker complex based machine learning (DCML) models for protein-ligand binding affinity prediction. *PLOS Computational Biology*, 18(4):1–17, 04 2022. doi: 10.1371/journal.pcbi.1009943. URL <https://doi.org/10.1371/journal.pcbi.1009943>.
- Loiseaux, D., Scoccola, L., Carrière, M., Botnan, M. B., and Oudot, S. Stable vectorization of multiparameter persistent homology using signed barcodes as measures. In *Thirty-seventh Conference on Neural Information Processing Systems*, 2023. URL <https://openreview.net/pdf?id=4mw0RQjAim>.
- MacLane, S. *Categories for the working mathematician*. Graduate Texts in Mathematics, Vol. 5. Springer-Verlag, New York-Berlin, 1971.
- Memar, P. and Faradji, F. A novel multi-class EEG-based sleep stage classification system. *IEEE Transactions on Neural Systems and Rehabilitation Engineering*, 26(1):84–95, 2017. URL <https://ieeexplore.ieee.org/document/8116601>.
- Mukherjee, S., Samaga, S. N., Xin, C., Oudot, S., and Dey, T. K. D-GRIL: End-to-end topological learning with 2-parameter persistence, 2024. URL <https://arxiv.org/abs/2406.07100>.
- Myers, A., Muñoz, D., Khasawneh, F. A., and Munch, E. Temporal network analysis using zigzag persistence. *EPJ Data Science*, 12(1):6, 2023. URL <https://epjdatascience.springeropen.com/articles/10.1140/epjds/s13688-023-00379-5>.
- Oreshkin, B. N., Amini, A., Coyle, L., and Coates, M. FC-GAGA: Fully connected gated graph architecture for spatio-temporal traffic forecasting. In *Proceedings of the AAAI conference on artificial intelligence*, volume 35, pp. 9233–9241, 2021. URL <https://ojs.aaai.org/index.php/AAAI/article/view/17114/16921>.
- Pearson, K. and Lee, A. On the laws of inheritance in man: I. inheritance of physical characters. *Biometrika*, 2(4): 357–462, 11 1903. ISSN 0006-3444. doi: 10.1093/biomet/2.4.357. URL <https://doi.org/10.1093/biomet/2.4.357>.
- Phan, H., Andreotti, F., Cooray, N., Chén, O. Y., and De Vos, M. SeqSleepNet: end-to-end hierarchical recurrent neural network for sequence-to-sequence automatic sleep staging. *IEEE Transactions on Neural Systems and Rehabilitation Engineering*, 27(3):400–410, 2019. URL <https://ieeexplore.ieee.org/document/8631195>.
- Rempe, D., Birdal, T., Zhao, Y., Gojcic, Z., Sridhar, S., and Guibas, L. J. Caspr: Learning canonical spatiotemporal point cloud representations. In Larochelle, H., Ranzato, M., Hadsell, R., Balcan, M., and Lin, H. (eds.), *Advances in Neural Information Processing Systems*, volume 33, pp. 13688–13701. Curran Associates, Inc., 2020. URL https://proceedings.neurips.cc/paper_files/paper/2020/file/9de6d14fff9806d4bcd1ef555be766cd-Paper.pdf.
- Riehl, E. *Categorical homotopy theory*. New Mathematical Monographs, Series Number 24. Cambridge University Press, 1914.
- Schäfer, P. and Leser, U. Multivariate time series classification with WEASEL+MUSE. *arXiv preprint arXiv:1711.11343*, 2017. URL <https://arxiv.org/pdf/1711.11343>.
- Scoccola, L., Setlur, S., Loiseaux, D., Carrière, M., and Oudot, S. Differentiability and optimization of multiparameter persistent homology. In *Proceedings of the 41st International Conference on Machine Learning*, volume 235 of *Proceedings of Machine Learning Research*, pp. 43986–44011. PMLR, 21–27 Jul 2024. URL <https://proceedings.mlr.press/v235/scoccola24a.html>.

- Supratak, A., Dong, H., Wu, C., and Guo, Y. DeepSleepNet: A model for automatic sleep stage scoring based on raw single-channel EEG. *IEEE transactions on neural systems and rehabilitation engineering*, 25(11):1998–2008, 2017. URL <https://ieeexplore.ieee.org/document/7961240>.
- Swenson, N., Krishnapriyan, A. S., Buluc, A., Morozov, D., and Yelick, K. PersGNN: Applying topological data analysis and geometric deep learning to structure-based protein function prediction. *arXiv preprint arXiv:2010.16027*, 2020. URL <https://arxiv.org/abs/2010.16027>.
- Tang, W., Long, G., Liu, L., Zhou, T., Blumenstein, M., and Jiang, J. Omni-scale CNNs: a simple and effective kernel size configuration for time series classification. In *International Conference on Learning Representations*, 2022. URL <https://openreview.net/forum?id=PDYs7Z2XFGv>.
- Tinarrage, R., Ponciano, J. R., Linhares, C. D. G., Traina, A. J. M., and Poco, J. ZigzagNetVis: Suggesting temporal resolutions for graph visualization using zigzag persistence. *IEEE Transactions on Visualization and Computer Graphics*, pp. 1–18, 2025. doi: 10.1109/TVCG.2025.3528197. URL <https://www.computer.org/csdl/journal/tg/5555/01/10844578/23zUk2J0sr6>.
- Vipond, O. Multiparameter persistence landscapes. *Journal of Machine Learning Research*, 21(61):1–38, 2020. URL <http://jmlr.org/papers/v21/19-054.html>.
- Wu, Z., Pan, S., Long, G., Jiang, J., Chang, X., and Zhang, C. Connecting the dots: Multivariate time series forecasting with graph neural networks. In *Proceedings of the 26th ACM SIGKDD international conference on knowledge discovery & data mining*, pp. 753–763, 2020. URL <https://dl.acm.org/doi/pdf/10.1145/3394486.3403118>.
- Xin, C., Mukherjee, S., Samaga, S. N., and Dey, T. K. GRIL: A 2-parameter Persistence Based Vectorization for Machine Learning. In *Proceedings of 2nd Annual Workshop on Topology, Algebra, and Geometry in Machine Learning (TAG-ML)*, volume 221 of *Proceedings of Machine Learning Research*, pp. 313–333. PMLR, 7 2023. URL <https://proceedings.mlr.press/v221/xin23a.html>.
- Yu, B., Yin, H., and Zhu, Z. Spatio-temporal graph convolutional networks: a deep learning framework for traffic forecasting. In *Proceedings of the 27th International Joint Conference on Artificial Intelligence*, pp. 3634–3640, 2018. URL <https://www.ijcai.org/proceedings/2018/0505.pdf>.
- Zhang, S., Mukherjee, S., and Dey, T. K. GEFL: Extended Filtration Learning for Graph Classification. In *Proceedings of the First Learning on Graphs Conference*, volume 198 of *Proceedings of Machine Learning Research*, pp. 16:1–16:26. PMLR, 09–12 Dec 2022. URL <https://proceedings.mlr.press/v198/zhang22b.html>.
- Zhao, Q., Ye, Z., Chen, C., and Wang, Y. Persistence enhanced graph neural network. In *Proceedings of the Twenty Third International Conference on Artificial Intelligence and Statistics*, volume 108 of *Proceedings of Machine Learning Research*, pp. 2896–2906. PMLR, 26–28 Aug 2020. URL <https://proceedings.mlr.press/v108/zhao20d.html>.
- Zhao, Y., Lin, X., Zhang, Z., Wang, X., He, X., and Yang, L. STDP-based adaptive graph convolutional networks for automatic sleep staging. *Frontiers in Neuroscience*, 17, 2023. ISSN 1662-453X. doi: 10.3389/fnins.2023.1158246. URL <https://www.frontiersin.org/journals/neuroscience/articles/10.3389/fnins.2023.1158246>.

A Formal definitions and proofs

There is a notion of proximity on the space of zigzag modules in terms of the *interleaving distance*. In Botnan & Lesnick (2018), the authors define interleaving distance between two zigzag modules by including them into $\mathbb{R}^{\text{op}} \times \mathbb{R}$ -indexed modules.

The interleaving distance on \mathbb{R}^n -indexed persistence modules is an extension of the same distance defined for \mathbb{R} -indexed persistence modules Chazal et al. (2009). We briefly recall the definition here. We refer the readers to Botnan & Lesnick (2018) for additional details.

Definition A.1 (*u-shift functor*). The *u*-shift functor $(-)_u: \mathbf{vec}^{\mathbb{R}^n} \rightarrow \mathbf{vec}^{\mathbb{R}^n}$, for $u \in \mathbb{R}^n$, is defined as follows:

1. For $M \in \mathbf{vec}^{\mathbb{R}^n}$, M_u is defined as $M_u(x) = M(x + u)$ for all $x \in \mathbb{R}^n$ and $M_u(x_1 \leq x_2) = M(x_1 + u \leq x_2 + u)$ for all $x_1 \leq x_2 \in \mathbb{R}^n$,
2. Let $M, N \in \mathbf{vec}^{\mathbb{R}^n}$. Let $F: M \rightarrow N$ be a morphism. Then, the corresponding morphism $F_u: M_u \rightarrow N_u$ is defined as $F_u(x) = F(x + u): M_u(x) \rightarrow N_u(x)$ for all $x \in \mathbb{R}^n$.

Definition A.2 (*ϵ -interleaving*). Let $M, N \in \mathbf{vec}^{\mathbb{R}^n}$. Let $\epsilon \in [0, \infty)$ be given. We will denote $(-)_{\epsilon}$ to be the shift functor corresponding to the vector $\epsilon = \epsilon(1, 1, \dots, 1)$. We say M and N are ϵ -interleaved if there are natural transformations $F: M \rightarrow N_{\epsilon}$ and $G: N \rightarrow M_{\epsilon}$ such that

1. $G_{\epsilon} \circ F = \varphi_M^{2\epsilon}$,
2. $F_{\epsilon} \circ G = \varphi_N^{2\epsilon}$,

where $\varphi_M^u: M \rightarrow M_u$ is the natural transformation whose restriction to each $M(x)$ is the linear map $M(x \leq x + u)$ for all $x \in \mathbb{R}^n$.

Definition A.3 (*Interleaving distance*). Let $M, N \in \mathbf{vec}^{\mathbb{R}^n}$. The interleaving distance $d_{\mathcal{I}}(M, N)$ between M and N is defined as

$$d_{\mathcal{I}}(M, N) := \inf\{\epsilon \geq 0: M \text{ and } N \text{ are } \epsilon\text{-interleaved}\}$$

and $d_{\mathcal{I}}(M, N) = \infty$ if there exists no interleaving.

We need the following two definitions to define interleaving distance between two zigzag modules.

Definition A.4 (*Left Kan Extension*). Let P and Q be two posets. Let $F: P \rightarrow Q$ be a functor. Let $P[F \leq q]$ denote the set $P[F \leq q] := \{p \in P: F(p) \leq q\}$. Given a persistence module $M: P \rightarrow \mathbf{vec}$, the *left Kan extension* of M along F is a functor $\text{Lan}_F(M): Q \rightarrow \mathbf{vec}$ given by

$$\text{Lan}_F(M)(q) := \text{colim} M|_{P[F \leq q]},$$

along with internal morphisms given by the universality of colimits.

Definition A.5 (*Block Extension Functor Botnan & Lesnick (2018)*). Let $\mathbb{U} \subset \mathbb{R}^{\text{op}} \times \mathbb{R}$ denote the poset $\mathbb{U} := \{(a, b): a \leq b\}$. Let $i: \mathbb{Z}\mathbb{Z} \rightarrow \mathbb{R}^{\text{op}} \times \mathbb{R}$ denote the inclusion. Let $(-)|_{\mathbb{U}}: \mathbf{vec}^{\mathbb{R}^{\text{op}} \times \mathbb{R}} \rightarrow \mathbf{vec}^{\mathbb{U}}$ denote the restriction. Then, the *block extension functor* $E: \mathbf{vec}^{\mathbb{Z}\mathbb{Z}} \rightarrow \mathbf{vec}^{\mathbb{U}}$ is defined as

$$E := (-)|_{\mathbb{U}} \circ \text{Lan}_i(\circ).$$

Definition A.6 (*Interleaving distance on zigzag modules*). Let M, N be two zigzag modules. Then

$$d_{\mathcal{I}}(M, N) := d_{\mathcal{I}}(E(M), E(N)).$$

We extend this definition of interleaving distance to quasi zigzag persistence modules. Let $\mathbb{U}\mathbb{U} \subset \mathbb{R}^{\text{op}} \times \mathbb{R} \times \mathbb{R}$ be the analog of \mathbb{U} , i.e. $\mathbb{U}\mathbb{U} := \{(a, b, c): a \leq b\}$. Let $\tilde{i}: \mathbb{Z}\mathbb{Z} \times \mathbb{Z} \rightarrow \mathbb{R}^{\text{op}} \times \mathbb{R} \times \mathbb{R}$ denote the inclusion. Then, define $\tilde{E} := (-)|_{\mathbb{U}\mathbb{U}} \circ \text{Lan}_{\tilde{i}}(\circ)$, analogous to the block extension functor.

Definition A.7. Let M, N be two quasi zigzag persistence modules. Then, the interleaving distance between M and N is given by

$$d_{\mathcal{I}}(M, N) := d_{\mathcal{I}}(\tilde{E}(M), \tilde{E}(N)).$$

Lemma A.8. \tilde{E} sends interval modules on $\mathbb{Z}\mathbb{Z} \times \mathbb{Z}$ to block interval modules.

This is analogous to Lemma 4.1 in Botnan & Lesnick (2018).

Lemma A.9. *Let M be a p.f.d quasi zigzag persistence module. If $M \cong \bigoplus_{k \in K} I_k$, then $\tilde{E}(M) \cong \bigoplus_{k \in K} \tilde{E}(I_k)$, where K is an indexing set.*

Proof. The functor $\text{Lan}_{\mathbb{I}}$ preserves direct sums MacLane (1971), as it is left-adjoint to the canonical restriction functor. The restriction functor also preserves direct sums. These two facts combined with Lemma A.8 give the result. \square

Definition A.10. Let $\mathbf{I}(\mathbb{ZZ} \times \mathbb{Z})$ denote the collection of all subposets in $\mathbb{ZZ} \times \mathbb{Z}$ such that their corresponding subposets in \mathbb{Z}^2 are intervals. Let M and N be two quasi zigzag persistence modules. The erosion distance is defined as:

$$d_{\mathcal{E}}(M, N) := \inf_{\epsilon \geq 0} \{ \forall I \in \mathbf{I}(\mathbb{ZZ} \times \mathbb{Z}), \\ \text{rk}^M(I) \geq \text{rk}^N(I^\epsilon) \text{ and} \\ \text{rk}^N(I) \geq \text{rk}^M(I^\epsilon) \}$$

Definition A.11. Let \mathcal{L} denote the collection of all worms in $\mathbb{ZZ} \times \mathbb{Z}$. Let M and N be quasi zigzag persistence modules. The erosion distance can be defined as:

$$d_{\mathcal{E}}^{\mathcal{L}}(M, N) := \inf_{\epsilon \geq 0} \{ \forall \boxed{\mathbf{p}}_{\delta}^2 \in \mathbf{I}(\mathbb{ZZ} \times \mathbb{Z}), \\ \text{rk}^M(\boxed{\mathbf{p}}_{\delta}^2) \geq \text{rk}^N(\boxed{\mathbf{p}}_{\delta+\epsilon}^2) \text{ and} \\ \text{rk}^N(\boxed{\mathbf{p}}_{\delta}^2) \geq \text{rk}^M(\boxed{\mathbf{p}}_{\delta+\epsilon}^2) \}.$$

Proposition 3.4. Given two quasi zigzag persistence modules M and N , $d_{\mathcal{E}}^{\mathcal{L}}(M, N) \leq d_{\mathcal{T}}(M, N)$ where $d_{\mathcal{T}}$ denotes the interleaving distance between M and N .

Proof. First, it is obvious that $d_{\mathcal{E}}^{\mathcal{L}}(M, N) \leq d_{\mathcal{E}}(M, N)$. Now, $d_{\mathcal{T}}(M, N) := d_{\mathcal{T}}(\tilde{E}(M), \tilde{E}(N))$. Let I be a subposet in $\mathbb{ZZ} \times \mathbb{Z}$ such that its corresponding subposet in \mathbb{Z}^2 is an interval. By Lemma A.8 and Lemma A.9, and the fact that generalized rank over a given subposet counts the number of intervals that contain the given subposet, we get $\text{rk}^M(I) = \text{rk}^{\tilde{E}(M)}(\tilde{i}(I) \cap \cup \cup)$. This gives us $d_{\mathcal{E}}(M, N) = d_{\mathcal{E}}(\tilde{E}(M), \tilde{E}(N))$. In Kim & Mémoli (2021), the authors show that $d_{\mathcal{E}}(V, W) \leq d_{\mathcal{T}}(V, W)$, where $V, W: \mathbb{R}^n \rightarrow \mathbf{vec}$ are \mathbb{R}^n -indexed persistence modules. Thus, we get $d_{\mathcal{E}}^{\mathcal{L}}(M, N) \leq d_{\mathcal{E}}(M, N) = d_{\mathcal{E}}(\tilde{E}(M), \tilde{E}(N)) \leq d_{\mathcal{T}}(\tilde{E}(M), \tilde{E}(N)) = d_{\mathcal{T}}(M, N)$. \square

Theorem 3.5. Let M and N be two quasi zigzag persistence modules such that $d_{\mathcal{T}}(M, N) = \epsilon$. Let \mathbf{p}, k be given. Let the ZZ-GRIL of M and N over $\boxed{\mathbf{p}}_{\delta}^2$ be denoted by λ^M and λ^N respectively. Then,

$$|\lambda^M(\mathbf{p}, k) - \lambda^N(\mathbf{p}, k)| \leq \epsilon.$$

Proof. We will show that $|\lambda^M(\mathbf{p}, k) - \lambda^N(\mathbf{p}, k)| = d_{\mathcal{E}}^{\mathcal{L}}(M, N)$.

To see $|\lambda^M(\mathbf{p}, k) - \lambda^N(\mathbf{p}, k)| \leq d_{\mathcal{E}}^{\mathcal{L}}(M, N)$, let $\lambda^M(\mathbf{p}, k) = \delta_M$ and $\lambda^N(\mathbf{p}, k) = \delta_N$. WLOG, assume $\delta_M \geq \delta_N$. Let $d_{\mathcal{E}}^{\mathcal{L}}(M, N) = \epsilon$. Therefore, by definition of $d_{\mathcal{E}}^{\mathcal{L}}$, we have $\text{rk}^M(\boxed{\mathbf{p}}_{\delta_M}^2) = k$ and $\text{rk}^M(\boxed{\mathbf{p}}_{\delta_N+\epsilon}^2) \leq \text{rk}^N(\boxed{\mathbf{p}}_{\delta_N}^2) = k$. Thus, by the definition of ZZ-GRIL, we get $\delta_N + \epsilon \geq \delta_M$, i.e., $\delta_M - \delta_N \leq \epsilon = d_{\mathcal{E}}^{\mathcal{L}}$.

To see $|\lambda^M(\mathbf{p}, k) - \lambda^N(\mathbf{p}, k)| \geq d_{\mathcal{E}}^{\mathcal{L}}(M, N)$, let $|\lambda^M(\mathbf{p}, k) - \lambda^N(\mathbf{p}, k)| = \epsilon$. Let $\boxed{\mathbf{p}}_{\delta}^2$ be a worm. Let $\text{rk}^N(\boxed{\mathbf{p}}_{\delta+\epsilon}^2) = k$. Then, $\lambda^N(\mathbf{p}, k) \geq \delta + \epsilon$. Thus, $|\lambda^M(\mathbf{p}, k) - \lambda^N(\mathbf{p}, k)| = \epsilon$ and $\lambda^N(\mathbf{p}, k) \geq \delta + \epsilon$ give $\lambda^M(\mathbf{p}, k) \geq \delta$. Therefore, $\text{rk}^M(\boxed{\mathbf{p}}_{\delta}^2) \geq k = \text{rk}^N(\boxed{\mathbf{p}}_{\delta+\epsilon}^2)$. Similarly, we can show $\text{rk}^N(\boxed{\mathbf{p}}_{\delta}^2) \geq \text{rk}^M(\boxed{\mathbf{p}}_{\delta+\epsilon}^2)$. Thus, by definition of $d_{\mathcal{E}}^{\mathcal{L}}$, we get that $|\lambda^M(\mathbf{p}, k) - \lambda^N(\mathbf{p}, k)| \geq d_{\mathcal{E}}^{\mathcal{L}}(M, N)$. \square

B Experimental Details

Here, we report additional details about our experiments. We begin by including a detailed description of the UEA datasets in Table 5. Further, we have a comparison of treating a multivariate time series as a sequence of point clouds versus treating it as a sequence of graphs as the input to the ZZ-GRIL framework. We report the results of this experiment in Table 4. We can see that there is no clear winner. On some datasets, ZZ-GRIL extracts more relevant information from sequences of point clouds while on some datasets, information from sequences of graphs performs better. We have

Dataset	Type	No. of series	Series length	No. of classes	Train size	Test size
FingerMovements	EEG	28	50	2	316	100
Heartbeat	AUDIO	61	405	2	204	205
MotorImagery	EEG	64	3000	2	278	100
NATOPS	HAR	24	51	6	180	180
SelfRegulationSCP2	EEG	7	1152	2	200	180

Table 5: Information about UEA Datasets used for experiments

a visualization of ZZ-GRIL in Figure 7. We can see in the figure that the ZZ-GRIL topological signature is different for samples of different classes and very similar for samples in the same class.

For all the experiments with sequence of point clouds, we choose a window size that is $\max(5, series_length//128)$ and overlap $\max(4, 0.7 * window_size)$. For the experiments with sequence of graphs, we choose a window size of $\min(series_length/5, 128)$ and an overlap of $0.7 * window_size$. Then, from the complete graph, we randomly choose a percentage between 65 and 75 of the edges depending on their weights. This is to ensure that the number of edges does not remain the same for all the graphs in the sequence. For all our experiments, we use 36 center points to compute ZZ-GRIL at. For model parameters, mostly, we use the same parameters as specified by the respective models Liu et al. (2024); Zhao et al. (2023). We notice that the training is sensitive to learning rate and we optimize the learning rate between $1e - 3$ and $5e - 5$ for different datasets.